



# Prediction of monthly Arctic sea ice concentration using satellite and reanalysis data based on convolutional neural networks

Young Jun Kim<sup>1</sup>, Hyun-cheol Kim<sup>2</sup>, Daehyeon Han<sup>1</sup>, Sanggyun Lee<sup>3</sup>, and Jungho Im<sup>1,4</sup>

<sup>1</sup>School of Urban and Environmental Engineering, Ulsan National Institute of Science and Technology, Ulsan, South Korea

5 <sup>2</sup>Unit of Arctic Sea-Ice Prediction, Korea Polar Research Institute, Incheon, Republic of Korea

<sup>3</sup>Centre for Polar Observation and Modelling, University College London, London, UK

<sup>4</sup>Environmental Resources Engineering, State University of New York College of Environmental Science and Forestry, Syracuse, NY, USA

10 *Correspondence to:* Jungho Im (ersgis@unist.ac.kr)

**Abstract.** Changes in Arctic sea ice affect atmospheric circulation, ocean current, and polar ecosystems. There have been unprecedented decreases in the amount of Arctic sea ice, due to the global warming and its various adjoint cases. In this study, a novel one-month sea ice concentration (SIC) prediction model is proposed, with eight predictors using a deep learning approach, Convolutional Neural Networks (CNN). This monthly SIC prediction model based CNN is shown to perform better  
15 predictions (mean absolute error (MAE) of 2.28%, root mean square error (RMSE) of 5.76%, normalized RMSE (nRMSE) of 16.15%, and NSE of 0.97) than a random forest (RF)-based model (MAE of 2.45%, RMSE of 6.61%, nRMSE of 18.64%, and NSE of 0.96) and a simple prediction model based on the yearly trend (MAE of 9.36%, RMSE of 21.93%, nRMSE of 61.94%, and NSE of 0.83) through hindcast validations. Spatiotemporal analysis also confirmed the superiority of the CNN model. The  
20 CNN model showed good SIC prediction results in extreme cases that recorded unforeseen sea ice plummets in 2007 and 2012 with less than 5.0% RMSEs. This study also examined the importance of the input variables through a sensitivity analysis. In both the CNN and RF models, the variables of past SICs were identified as the most sensitive factor in predicting SIC. For both models, the SIC-related variables generally contributed more to predict SICs over ice-covered areas, while other meteorological and oceanographic variables were more sensitive to the prediction of SICs in marginal ice zones. The proposed one-month SIC prediction model provides valuable information which can be used in various applications, such as Arctic  
25 shipping route planning, management of fishery industry, and long-term sea ice forecasting and dynamics.

## 1 Introduction

Sea ice refers to the frozen seawater that covers approximately 15% of the oceans in the world (National Snow and Ice Data Center, 2018). Sea ice reflects more solar radiation than the water's surface, which makes the polar regions relatively cool. Sea ice shrinks in summer due to the warmer climate and expands in the winter season. Many studies on Arctic sea ice  
30 monitoring and dynamics have been conducted because it plays a significant role in the energy and water balance of global climate systems (Ledley, 1988; Guemas et al., 2014). In particular, the change in sea ice is an important indicator that hows



the degree of on-going climate change (Johannessen et al., 2004). Global warming causes a decrease in sea ice that worsens the arctic amplification, which in turn accelerates global warming itself (Cohen et al., 2014; Francis and Vavrus, 2015). In addition, sea ice affects various oceanic characteristics and societal issues, such as ocean current circulation, by changing salinity and temperature gradation (Timmermann et al., 2009); polar ecosystems, by affecting key parts of the Arctic food web like sea-ice algae (Doney et al., 2011); and economic industries e.g., Arctic shipping routes (Melia et al., 2016).

Arctic sea ice has been rapidly declining, which impacts not only the Arctic climate, but also mid-latitudes (Yu et al., 2017). Numerous studies have shown significant interactions between ocean and climate characteristics, such as sea surface temperature, solar radiation, surface temperature, and the changes of sea ice (Guemas et al., 2014). Therefore, the prediction of long and short-term sea ice change is an important issue in forecasting climate change (Yuan et al., 2016). Various approaches, including numerical modeling and statistical analysis, have been proposed to develop models to predict sea ice characteristics (Guemas et al., 2014; Chi and Kim, 2017). Many of the studies have adopted statistical models using *in situ* observations or reanalysis data based on the relationship between sea ice and ocean/climate parameters (Comeau et al., 2019). However, the literature has reported that sea ice prediction is a very challenging task under the changing Arctic climate system (Holland et al., 2010; Stroeve et al., 2014). Chi and Kim (2017) suggested a deep-learning based model using Long and Short-Term Memory (LSTM) in comparison to a traditional statistical model. Their model showed good performance in the one-month prediction of sea ice concentration (SIC), with less than 9% average monthly prediction errors. However, it had low predictability during the melting season (RMSE of 11.09% from July to September). Kim et al. (2018) proposed a near-future SIC prediction model (10-20 years) using deep neural networks together with the Bayesian model averaging ensemble, resulting in a root mean square error (RMSE) of 19.4% on annual average. This study suggests that deep learning techniques are good to connect variables under non-linear relationships, such as SIC and climate variables. However, this study also showed low prediction accuracy during the melting season (nRMSE of 102.25% from June to September). Wang et al. (2017) used convolutional neural networks (CNN) to estimate SIC in the Gulf of Saint Lawrence from synthetic aperture radar (SAR) imagery. Their study compared their CNN model to a multilayer perceptron (MLP) model, showing the superiority of the CNN model in SIC estimation with an RMSE of about 22%.

However, the previous studies have focused on the long-term prediction of SIC using deep learning techniques (i.e., over one-year prediction). Studies regarding short-term sea ice forecasting have received relatively little attention (Grumbine, 1998; Preller and Posey, 1989). The short-term forecasting of sea ice conditions is also important for maritime industries and decision making on field logistics (Schweiger and Zhang, 2015). In addition, there is room to further improve the accuracy of short-term SIC prediction models with more advanced techniques and data. SIC describes the amount of the sea that is covered by ice (Fritzner et al., 2018), and it has been widely used as a simple and intuitive proxy to identify the characteristics of sea ice. Thus, this study aimed to predict the changes in Arctic sea ice characteristics using SIC.

This study proposes a novel deep learning-based method to predict SIC based on the predictors of spatial patterns, considering



65 the operational forecast of sea ice characteristics. The objectives of this study were to (1) develop a novel monthly SIC prediction model using a deep learning approach, CNN; (2) examine the prediction performance of the proposed model through comparison with a random forest-based SIC prediction model; and (3) conduct a sensitivity analysis of predictors that affect SIC predictions.

## 2. Data

70 Three types of datasets were used in this study, which document sea ice concentrations, oceanographic, and meteorological characteristics in the Arctic. This study focuses on the prediction accuracy of the proposed models as well as the sensitivity of each predictor on monthly SIC prediction. The spatial domain of this study is a region of the Arctic Ocean (180°W – 180°E / 40°N – 90°N), and the temporal coverage is the 30 years between 1988 and 2017.

75 The first dataset is the daily sea ice concentration observation data, obtained from the National Snow and Ice Data Center (NSIDC), which is derived from the Nimbus 7 Scanning Multichannel Microwave Radiometer (SMMR) and the Defense Meteorological Satellite Program (DMSP) Special Sensor Microwave Imager (SSM/I and SSMIS). The second dataset is the daily sea surface temperature data, obtained from National Oceanic and Atmospheric Administration (NOAA) Optimal Interpolation Sea Surface Temperature (OISST) version 2, which is constructed from Advanced Very High-Resolution Radiometer (AVHRR) observation data with 0.25° resolution from 1988 to 2017. The third dataset is the monthly European Centre for Medium-Range Weather Forecasts (ECMWF) Re-Analysis Interim (ERA-Interim) data, which is used in order to  
80 build predictors for one-month SIC prediction, including the surface air temperature, albedo, and v-wind vector in 0.125°.

In this study, a total of eight predictors were selected and used to predict SIC next month (Table 1) based on the literature and a preliminary statistical analysis of potential predictors. The predictors are: SIC one-year before (sic\_1y), SIC one-month before (sic\_1m), SIC anomaly one-year before (ano\_1y), SIC anomaly one-month before (ano\_1m), sea surface temperature (SST), 2-meter air temperature (T2m), forecast albedo (FAL), and the amount of v-wind (v-wind).

85 **Table 1.** The specifications of the eight predictors used to predict short-term SIC in the study.

Variable	Source	Unit	Temporal resolution	Spatial resolution	Normalization
SIC one-year before (sic_1y)	NSIDC	%	Daily	25km	0 - 1
SIC one-month before (sic_1m)	NSIDC	%	Daily	25km	0 - 1
SIC anomaly one-year before (ano_1y)	NSIDC	%	Daily	25km	-1 - 1
SIC anomaly one-month before (ano_1m)	NSIDC	%	Daily	25km	-1 - 1
Sea surface temperature one-month before (SST)	NOAA OISST ver.2	K	Daily	0.25°	0 - 1



2-meter air temperature one-month before (T2m)	ECMWF ERA Interim	K	Monthly	0.125°	0 - 1
forecast albedo one-month before (FAL)	ECMWF ERA Interim	%	Monthly	0.125°	0 - 1
the amount of v-wind one-month before (v-wind)	ECMWF ERA Interim	m/s	Monthly	0.125°	0 - 1

In order to have the same spatial and temporal scales, the daily data, including SIC and SST, were transformed into monthly-means and onto a polar stereographic projection with 25km grids. The predictors were normalized into 0 to 1 or -1 to 1 (for ano\_1y and ano\_1m). Since sea ice decline has accelerated in recent years, especially in the summer season (Stroeve et al, 2008; Schweiger et al., 2008; Chi and Kim, 2017), we computed the SIC anomaly variables only for a more recent time period (2001-2017) rather than the entire study period (1988-2017). This was done in order to focus on the trends in recent sea ice changes. The v-wind indicates the relative amount of wind towards the North Pole: the larger the v-wind, the more it blows from South to North. The v-wind data were derived using an 11-by-11 moving window based on a mean function from the raw 10-meter-height v-wind vector data. Regarding the moving window, this study set the analysis unit as an 11-by-11 window (neighboring 5 pixels; about 125 km) in order to consider the synoptic-scaled climate and ocean circulation in the polar region (Crane, 1978; Emery et al., 1997).

The eight predictors selected in this study have theoretical backgrounds that are related to the characteristics of SIC. First, SIC itself can affect the SIC in the future because it has a clear inter-annual trend through the melting and freezing seasons (Deser and Teng, 2008; Chi and Kim, 2017). It is a useful characteristic when conducting a time-series analysis, and thus, two SIC time-series climatology predictors (SIC one-year before and SIC one-month before) were used in this study. Further, we used two supplementary predictors that indicate the anomalies of SIC one-year before and SIC one-month before, in order to consider anomalous sea ice conditions in the models. Second, changes in SST and SIC have a significant relationship with each other, with regards to the heat budget (Rayner et al., 2003; Screen and et al., 2013; Prasad et al., 2018). The re-emergence of sea ice anomalies are also partially explained by the persistence of SST anomalies (Guemas et al., 2014). Air temperature and albedo are related to the amount of solar radiation enabling the prediction of SIC changes. The solar radiation heats the surface of the ocean as well as the sea ice. This causes a rise in the SST while also reducing albedo on the sea ice by melting the surface snow or thinning the sea ice (Screen and Simmonds, 2010; Mahajan et al., 2011). Moreover, the surface snow melting produces melt ponds, wet sea-ice surfaces, and wet snow cover (Kern et al., 2016). Warm winds from lower latitudes toward the Arctic can also reduce sea ice (Kang et al., 2014) and local wind forces affect the sea ice motion and formation (Shimada et al., 2006).



### 3. Methods

#### 3.1 Prediction models: Convolutional Neural Networks (CNN), Random Forest (RF), and simple prediction model

This study proposes a SIC prediction model using a Convolutional Neural Network (CNN) deep learning approach. CNN is a kind of artificial neural network (ANN) model first suggested by LeCun et al. (1998) and has since been further developed with various structures and algorithms (Deng et al., 2013). Many studies have adopted CNN approaches to complete image recognition or classification tasks (Browne and Ghidary, 2003; Deng et al., 2013; Ren et al., 2015; Zhang et al., 2019). CNN learns the features of images, and takes them into account as key information, in order to extract outputs (Wang et al., 2017). Convolutional networks share their weights and connect neighboring layers using convolution layers like neurons (Wang et al., 2016). The convolutional structure is a unique feature of CNN models that often shows higher performance than other types of ANN in image recognition studies (Krizhevsky et al., 2012; Lee et al., 2009). The basic CNN structure consists of a bundle of convolutional layers, a number of pooling layers, and a fully connected layer. The convolutional process is to generate feature maps from gridded input data with kernel and activation functions. A CNN model extracts the best feature map from an input image through an iterative training process including backpropagation learning and an optimization algorithms.

In CNN approaches, when 3-dimensional data (i.e., width, height, and depth (or channel)) are entered, several moving kernels pass through the data for each channel and transform them into feature maps using dot-product calculation. Through a number of convolutional processes, the model uses the fully connected layer to generate the final answer. The series of convolutional processes involved in this process require significant computation loads. To prevent heavy computation, both the stride (i.e., how to shift a moving kernel) and the pooling (i.e., how to conduct downsampling) techniques are widely used, which make the size of the input data in the following convolutional process reduced. To avoid too much data reduction, many studies have adopted a padding technique, which covers input data with extra dummy values (Wang et al., 2016). The feature map achieved through the convolutional process is a convolved map that contains a higher level of features of an image (Chen et al., 2015). In general, a CNN model contains larger learning capacity and provides more robustness against noise than normal MLP models because of the more trainable parameters as well as the structure of deeper networks (Wang et al., 2017).

In order to conduct a quantitative comparison of the prediction performance of the proposed CNN model, this study used random forest (RF), which is an ensemble-based machine learning technique (Yoo et al., 2018). The RF model was used to solve image-based classification problems such as the building extraction, land-cover classification, and crop classification (Liu et al., 2018; Guo and Du, 2017; Forkuor et al., 2018; Sonobe et al., 2017). RF extracts features using classifiers of each variable (Liu et al., 2018). The user can deal with two main parameters: the number of decision trees and the number of split variables at the nodes (Ghimire et al., 2010). In this study, we used 50 trees and 11 random variables to be used in the decision split because random selection using one-third of variables in each split has been used widely in solving regression problems



(Mutanga et al., 2012; Chu et al., 2014). Compared to the CNN approach, RF has a relatively low learning capacity from the perspective of the parametric size.

145 Lastly, a simple climatology based prediction model was also examined using a simple linear extrapolation. Since sea ice shows a clear climatological pattern (Parkinson and Cavalieri, 2002; Deser and Teng, 2008; Chi and Kim, 2017), this study predicted SICs for each month using the yearly trends of SICs. This study used the climatology based simple prediction model along with the RF as baseline models to figure out the performance of the CNN model for SIC prediction.

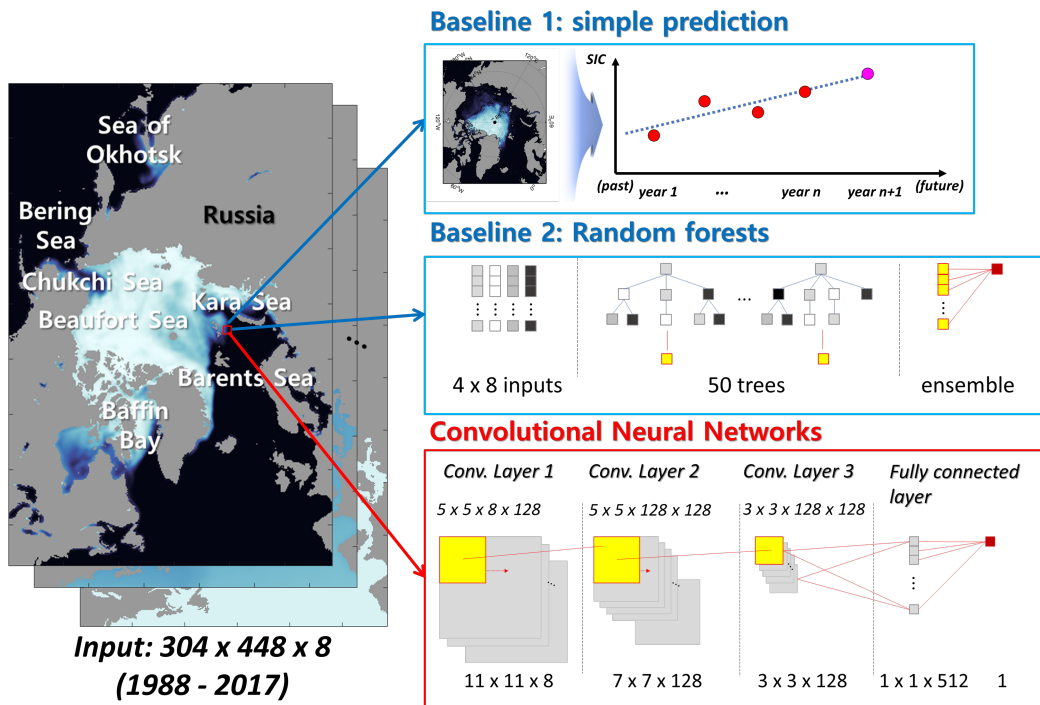
### 3.2 Research Flow

This study examined three models in order to predict SIC using the simple climatology and RF-based (baselines) and CNN-  
150 based approaches (Fig. 1). We designed twelve individual models (i.e., monthly models) to predict SIC for each month. A hindcast validation approach was used to evaluate each model's performance. Each monthly model was trained using the past data starting from 1988. For instance, 12-years' data (1988-1999) and 29-years' data (1988-2016) were trained to predict SICs in 2000 and 2017, and 2000 and 2017 SIC data were used as validation data, respectively. Eight input data during the past 30 years that consist of 304 \* 448 sized grids were used as training data in the RF and CNN models. In the case of the RF model,  
155 an additional 24 input parameters, along with the eight predictors, were considered. They are the mean, minimum, and maximum values of each predictor calculated using a 11-by-11 window. These additional variables for RF are to fill the conceptual gaps between the two approaches by considering the spatial patterns of predictors such as features in the CNN model. Since most SIC samples were biased to zero values because of the numerous pixels in the open sea, the training samples were balanced out considering the SIC values (0 – 100%) using a monthly maximum sea ice extent mask, which shows the  
160 widest sea ice extent during the entire study period (1988-2017) for each month. As a result, in case of 2017, about 600,000 samples on average (i.e., from about 400,000 samples in Sep. to about 850,000 samples in Mar.) were trained for both monthly models (i.e., RF and CNN). However, the unbalance sampling problem still remained because the lower SIC (less than 40%) samples were relatively small (about 20% of the entire training samples). In case of the simple prediction model, the SICs of each pixel was predicted using only yearly-climatologies from 1988. For example, SICs in Jan. 2000 were predicted using  
165 linear extrapolation from SICs of Januarys during 1988-1999 by grid.

As described in Fig. 1, the CNN model consists of three convolutional layers and one fully connected layer. Wang et al. (2017) used CNNs to estimate SIC from SAR data, and showed that the use of three convolutional layers performed better than one or two layers. In this study, the root mean square propagation (RMSProp) optimizer with a learning rate of 0.001, and the relu activation function were used in the model. The RMSProp optimizer has a similar process to a gradient descent algorithm  
170 which divides the gradients by a learning rate (Tieleman and Hinton, 2012). Fifty (50) epochs with a batch size as 1,024 were used in the proposed CNN model. The best model showing the highest prediction accuracy in validation during the training process was selected and used for further analysis. The CNN model was implemented using the Tensorflow Keras open-source

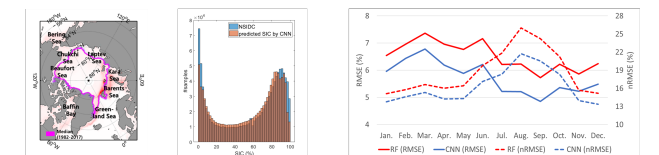


library, while the simple prediction and RF models were implemented using the interp1 and TreeBagger functions in the MATLAB r2018a, respectively.



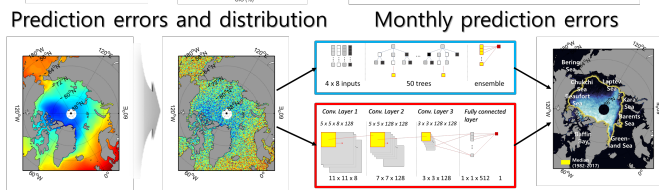
**Prediction accuracy**

Comparison of prediction accuracy and spatio-temporal analysis



**Variable sensitivity**

Examination of variable sensitivity of both models



**Extreme cases**

Analysis of extreme cases: September 2007 and 2012

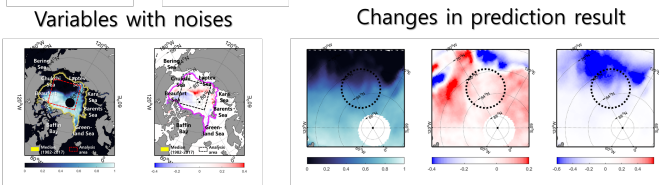


Figure 1. Study area and research flow.



This study firstly evaluated the model performance by quantitatively comparing the prediction results of the three models based on four accuracy metrics: mean absolute error (MAE, Eq. (1)), root mean square error (RMSE, Eq. (2)), normalized root mean square error (nRMSE, Eq. (3)), and Nash-Sutcliffe efficiency (NSE, Eq. (4)). In the melting season, many pixels contain relatively low SIC values compared to the freezing season. By dividing the RMSE by the standard deviation of actual SICs, the nRMSE can represent the prediction accuracy considering the range of SIC values (Kim et al., 2018). The NSE is a widely-used measure of prediction accuracy (Moriasi et al., 2007). It can provide comprehensive information regarding data by comparing the relative variance of prediction errors and variance of the observation data (Nash and Sutcliffe, 1970; Moriasi et al., 2007). The NSE has a range from  $-\infty$  to 1.0. A model is more accurate when the NSE value closer to 1, but unacceptable when the value is negative (Moriasi et al., 2007).

$$MAE = \text{mean}(|\text{predicted SIC} - \text{actual SIC}|) \quad (1)$$

$$RMSE = \sqrt{\text{mean}[(\text{predicted SIC} - \text{actual SIC})^2]} \quad (2)$$

$$nRMSE = \frac{\sqrt{\text{mean}[(\text{predicted SIC} - \text{actual SIC})^2]}}{\text{std}(\text{actual SIC})} \quad (3)$$

$$NSE = 1 - \frac{\Sigma(\text{actual SIC} - \text{predicted SIC})^2}{\Sigma(\text{actual SIC} - \text{mean}(\text{actual SIC}))^2} \quad (4)$$

With respect to prediction accuracy analysis, a specific mask that covers only pixels that have shown sea ice more than once in the past 10 years was used to prevent an inflation of overall accuracy that may have happened due to the effect of pixels on open seas in the melting season (Chi and Kim, 2017; Kim et al. 2018). For example, to calculate the prediction accuracy of predicted SIC in January 2017, the mask covered only pixels that have shown sea ice in Januarys from 2007 to 2016. To examine prediction performance in the marginal sea ice zone, the models were compared in two cases: all range of SICs (0-100%) and low SICs (0-40%).

In addition, the study examined the spatial distribution maps showing the annual MAE of three models during 2000-2017. The spatial relationship between SIC anomalies and prediction errors was also explored. Since the actual anomalies, as well as actual prediction errors (predicted SICs – actual SICs), tended to cancel each other out by averaging negative and positive values, we used absolute anomaly and error values. The distribution of predicted SICs by both models was also compared for the melting season (Jun. – Sep.). Further, the averaged monthly trends of prediction accuracy using RMSE and nRMSE together were examined with the trends of annual mean nRMSE by dividing the data into melting (Jun. – Sep.) and freezing (Dec. – Mar.) seasons.

In this research, we compared and examined prediction results focusing on two extreme cases of SIC: September 2007 and 2012. There was unexpectedly large Arctic sea ice shrinkage in summer 2007 and 2012 because of the large-scale changes in climate conditions and August cyclones, respectively (Devasthale et al., 2013). Therefore, for detailed analysis, visual



interpretation comparing the spatial patterns of prediction errors and input variables was conducted by focusing on the regions showing high prediction errors in Sep. 2007 and Sep. 2012.

210 Lastly, we examined the variable sensitivity for each model. Rodner et al. (2016) evaluated the variable sensitivity of built-in CNN architectures in three ways: adding random Gaussian noises, taking geometric perturbations, and setting random impulse  
215 noises (i.e., set the pixel values to zero) to input images. In this research, variable sensitivity analysis was conducted using their first and third methods. To examine the influence of variables on prediction accuracy, we added random Gaussian noises with zero-mean and 0.1 standard deviation, then compared any changes of RMSE for each variable (Eq. (5)). In addition, to examine the spatial effects on the predictions, the prediction results were compared by setting zero values for two groups of variables: sea ice related variables (sic\_1y, sic\_1m, ano\_1y, and ano\_1m) and other environmental variables (SST, T2m, FAL, and v-wind).

$$\text{Sensitivity } (Var_x) = \frac{\text{Changed RMSE with variable } x \text{ containing noises}}{\text{Original RMSE}} \quad (5)$$

## 4. Results and Discussion

### 4.1 Monthly prediction of SIC

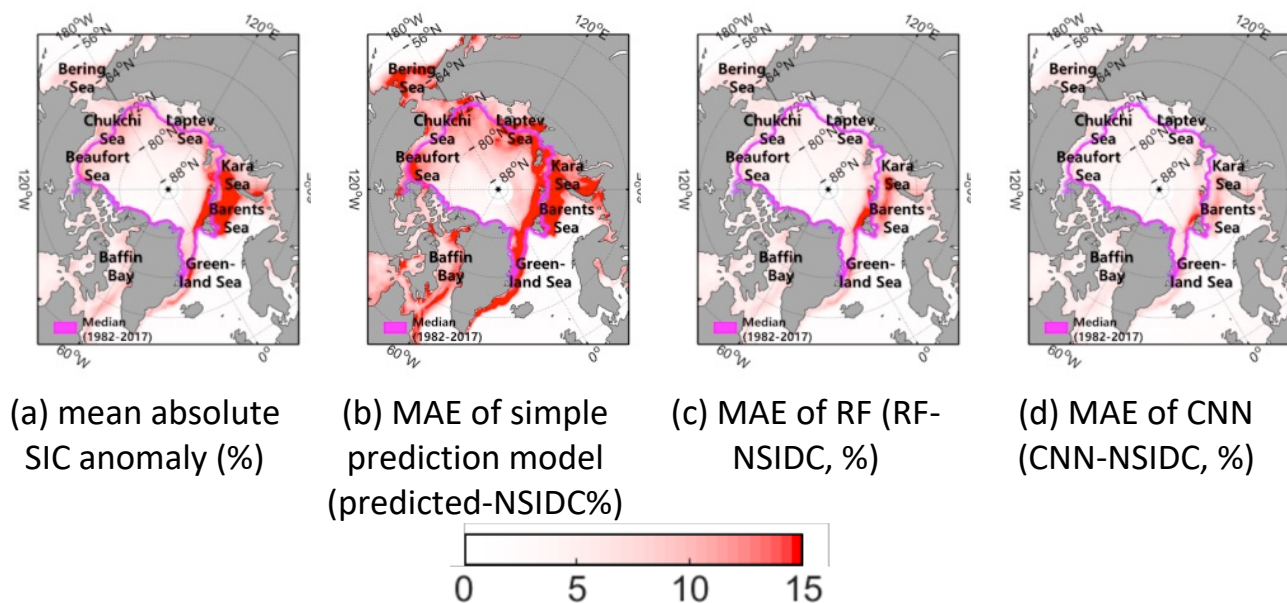
220 Table 2 shows the average prediction accuracies of the models during 2000-2017. The CNN model showed higher performance than the simple prediction as well as RF models in all accuracy metrics. When it comes to considering all range of SICs (0-100%), the simple prediction model resulted in the lowest prediction performance (MAE of 9.36%, RMSE of 21.93%, nRMSE of 61.94%, and NSE of 0.83). While the RF and CNN models resulted in good prediction accuracy with a small difference in MAE and RMSE (CNN: MAE of 2.28%, RMSE of 5.76%, and NSE of 0.97; RF: MAE of 2.45%, RMSE of 6.61%, and NSE of 0.96), the CNN model showed better results than the RF model for nRMSE (16.15% and 18.64%, respectively). These  
225 results imply that the error distribution of the CNN model was more stable than the simple prediction model as well as RF. In comparison at low SICs (0-40%), the MAE increased but it was due to the lower SIC values. The RMSE and nRMSE of the simple prediction model have decreased, but the others increased (simple model: 11.96%; RF: 7.23%; and CNN: 6.18%). It implies that the RF and CNN models might be relatively weak to predict SICs in the marginal sea ice zone when compared to the central zone. The NSE values decreased for all models for low SICs (simple model: from 0.93 to 0.60; RF: from 0.96 to  
230 0.90; and CNN: from 0.97 to 0.93). Nonetheless, the CNN model produced consistently higher performance than the other models for both cases.



**Table 2.** Average prediction accuracies among three models on every SIC (0-100%) and low SICs (0-40%) during 2000-2017 (mean absolute error, root mean square errors, normalized root mean square errors, and Nash-Sutcliffe efficiency).

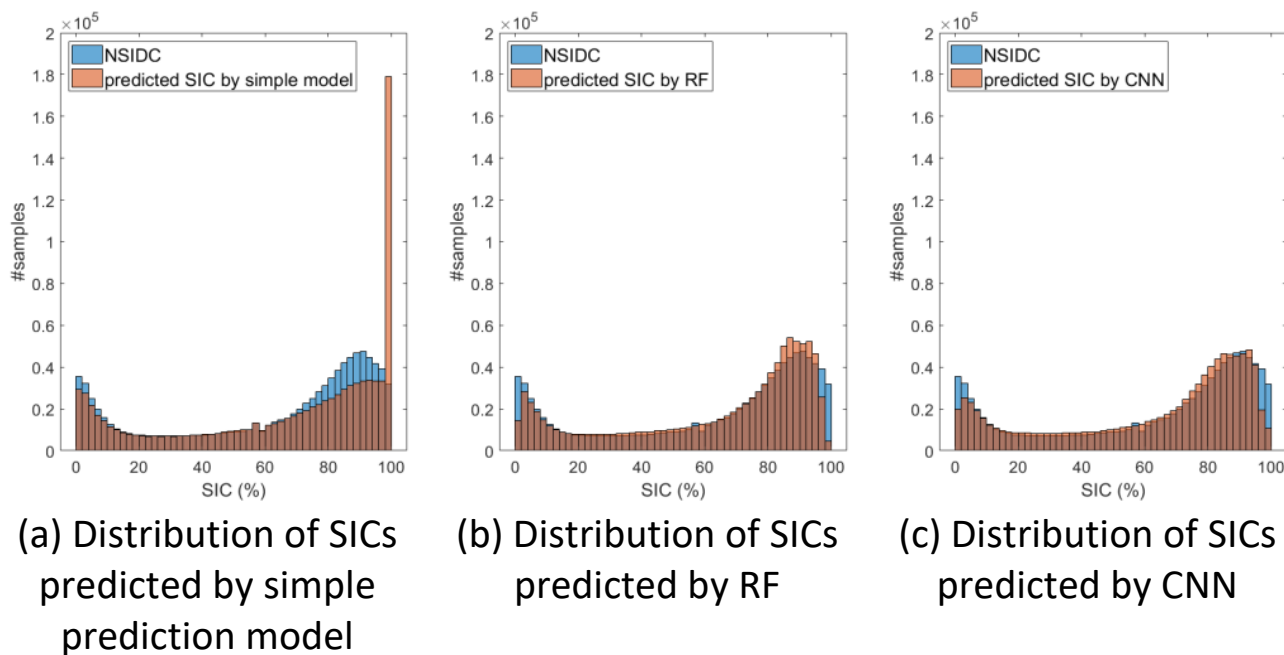
		MAE	RMSE	nRMSE	NSE
All range of SICs (0-100%)	Simple prediction	9.36%	21.93%	61.94%	0.83
	RF	2.45%	6.61%	18.64%	0.96
	CNN	2.28%	5.76%	16.15%	0.97
Low SICs (0-40%)	Simple prediction	3.88%	11.96%	33.22%	0.60
	RF	2.38%	7.23%	19.87%	0.90
	CNN	2.13%	6.18%	16.87%	0.93

235 The spatial distribution of the annual MAE of both models during 2000-2017 is shown in Fig. 2. From visual inspection, it can be seen that the prediction errors were dominant in the marginal areas (i.e., the boundaries between the sea ice and open seas). In particular, high prediction errors appeared around the Kara Sea and the Barents Sea (Fig. 2a). The Pearson's correlation coefficients between the absolute sea ice anomalies and the absolute errors are 0.87, 0.88, and 0.86 ( $p < 0.01$ ) for the simple model, RF, and CNN, respectively. Since the marginal sea ice, particularly thin ice, is susceptible to change (Stroeve et al., 2008; Chevallier et al., 2013; Zhang et al., 2013), the prediction accuracy may have decreased. Weak predictability on the marginal sea ice zone might be due to relatively small training sample size over the area. Further, the region from the Kara Sea to the Barents Sea shows consistent sea ice retreats because of inflows of warm and salty ocean water from the Atlantic Ocean into the Barents-Kara Sea (Schauer et al., 2002; Áρθun et al., 2012; Kim et al., 2018) and cumulative positive solar radiation in the summer season (Stroeve et al., 2012). Using a visual comparison, it can be seen that the degree of errors is higher in RF than in CNN (Fig. 2b-c).



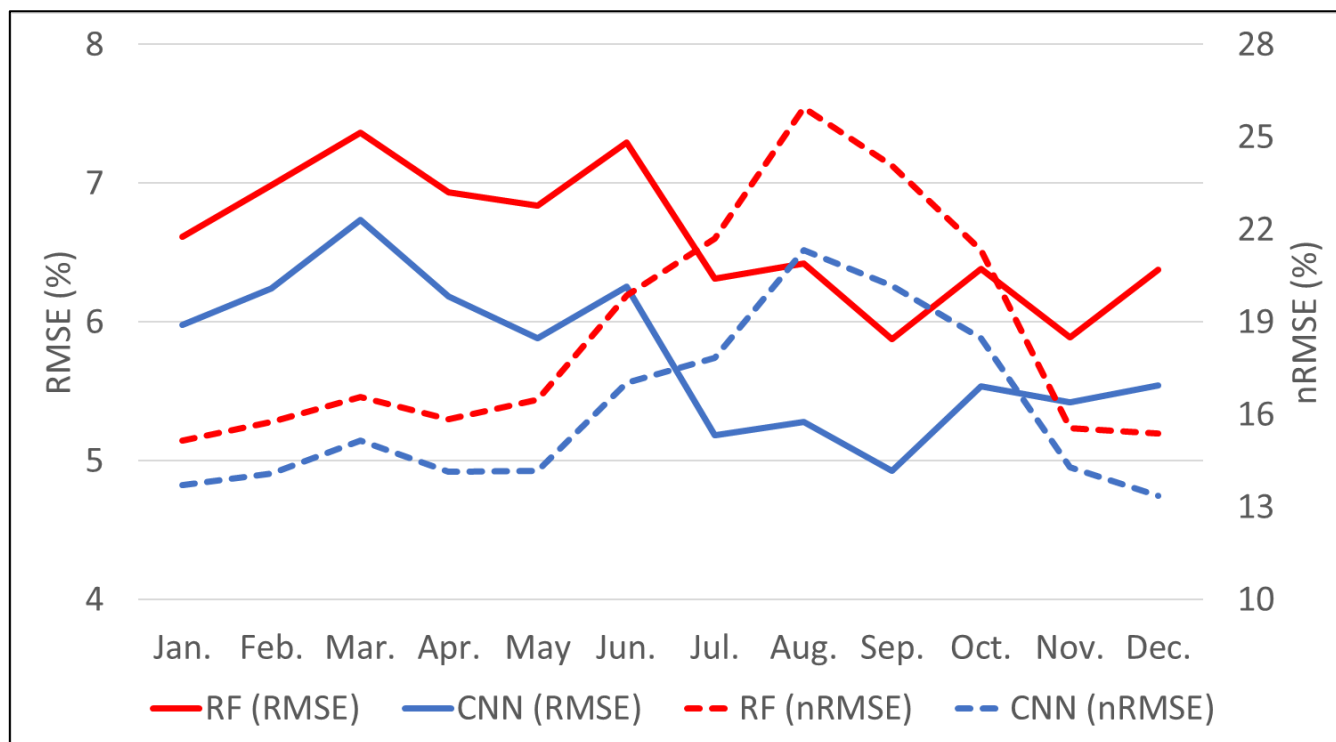
**Figure 2.** The mean absolute SIC anomaly (a) and mean absolute errors between predicted SICs and the actual SICs by the simple prediction model (b), RF (c) and CNN (d) during 2000-2017.

Figure 3 shows the histograms of NSIDC SICs and the predicted SICs by three models in the melting season (Jun. – Sep.) during 2000-2017. The simple prediction model predicted higher SICs as 100% (Fig. 3a). It implies that the linear trend-based model tended to over-estimate SICs in the melting season. The model did not catch well the decreasing trends of sea ice due to global warming. On the other hand, the RF and CNN models showed relatively weak predictability for boundary SIC values (i.e., less than 10% and over 90% SICs). In particular, the RF model showed a weakness to predict SICs near zero (0%) and 100%. By focusing on the RF and CNN models, the mean and standard deviation values of prediction errors (predicted SIC - NSIDC) were examined for lower as well as higher SICs. In the case of lower SICs (less than 5%), both models showed over-estimation. In detail, the CNN model showed a better prediction result than RF (CNN: mean error of 4.84% and std. of 7.65%; RF: mean error of 5.92% and std. of 9.77%). On the other hand, in the case of higher SICs (over 95%), both models showed under-estimation. The RF model shows -4.62% of error and 4.57% of standard deviation, but the CNN shows -4.17% and 4.14%, respectively. With the same training samples, the CNN resulted in higher prediction accuracy on both lower and higher SICs. It might be because of the larger learning capacity of CNN than RF (Wang et al., 2017).



**Figure 3.** Histograms of SICs based on NSIDC (blue) and three models (red) in the melting season (Jun. – Sep.) during 2000-2017.

Since the simple prediction model did not work well when compared to the RF and CNN models, the subsequent analyses are focused on the RF and CNN models. Figure 4 shows monthly prediction accuracies (i.e., RMSE and nRMSE) for the RF and the CNN models. The RF model showed lower prediction accuracy than the CNN model for all months. With regards to the RMSE of the CNN model, the prediction accuracy was higher in the melting season (Jun. – Sep.; 5.41%) than in the freezing season (Dec. – Mar.; 6.13%). However, as mentioned, the RMSE considers the range of sample values; for instance, more zero or low SIC values were found in the melting season (Chi and Kim, 2017). Thus, the nRMSE showed the opposite pattern to the RMSE. The normalized RMSE using the standard deviation can show the prediction accuracy considering the different ranges of SIC by month. In nRMSE of the CNN model, there is a different pattern between the melting season (Jun. – Sep.; 19.09%) and freezing season (Dec. – Mar.; 14.08%). According to the two-sample t-test, the nRMSE in melting season is higher than in freezing season ( $p < 0.01$ ;  $n = 18$ ) throughout the entire period (2000-2017). The difficulty of SIC prediction in the melting season is a well-known problem because of the unexpected decline of Arctic sea ice in recent years (Stroeve et al., 2007; Chi and Kim, 2017).



275

**Figure 4.** Monthly prediction accuracies with differences between two models for the entire periods (2000-2017, RMSEs and nRMSEs).

By focusing on the different patterns of prediction accuracy in the freezing (Dec. – Mar.; nRMSE of 14.08%) and melting season (Jun. – Sep.; nRMSE of 19.09%), the yearly trends in the prediction accuracy of the CNN model were examined (Fig. 5). The nRMSE in the melting season showed an increasing trend in more recent years (2000-2017). Since the dynamic changes in the Arctic environment, including warm air temperature (Hassol, 2004; Zhang et al., 2007), thinning sea ice (Maslanik et al., 2007), higher ocean surface temperature (Steele et al., 2008) have intensified in recent years, it makes the prediction of SIC in the melting season much more challenging. For instance, the Arctic sea ice extent experienced two major plummets, one in summer 2007, and one in summer 2012 because of multiple causes, such as the unexpected warm atmospheric conditions, radiation anomalies, and summer cyclones (Kauker et al., 2009; Kay et al., 2008; Parkinson and Comiso, 2012; Zhang et al., 2013).

285

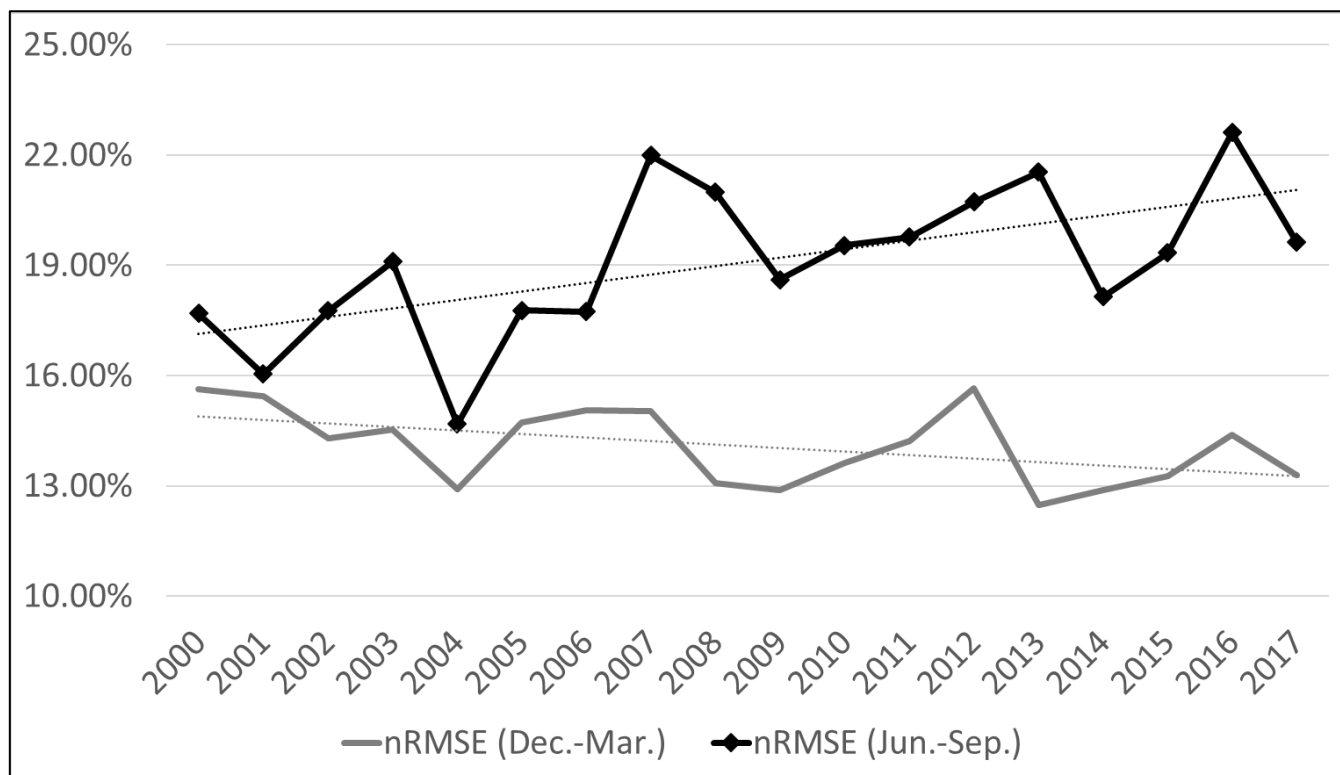


**Figure 5.** Changes of prediction accuracy (nRMSE) using CNN model in freezing (Dec.-Mar.) and melting (Jun.-Sep.) season (2000-2017, dotted lines show trend).

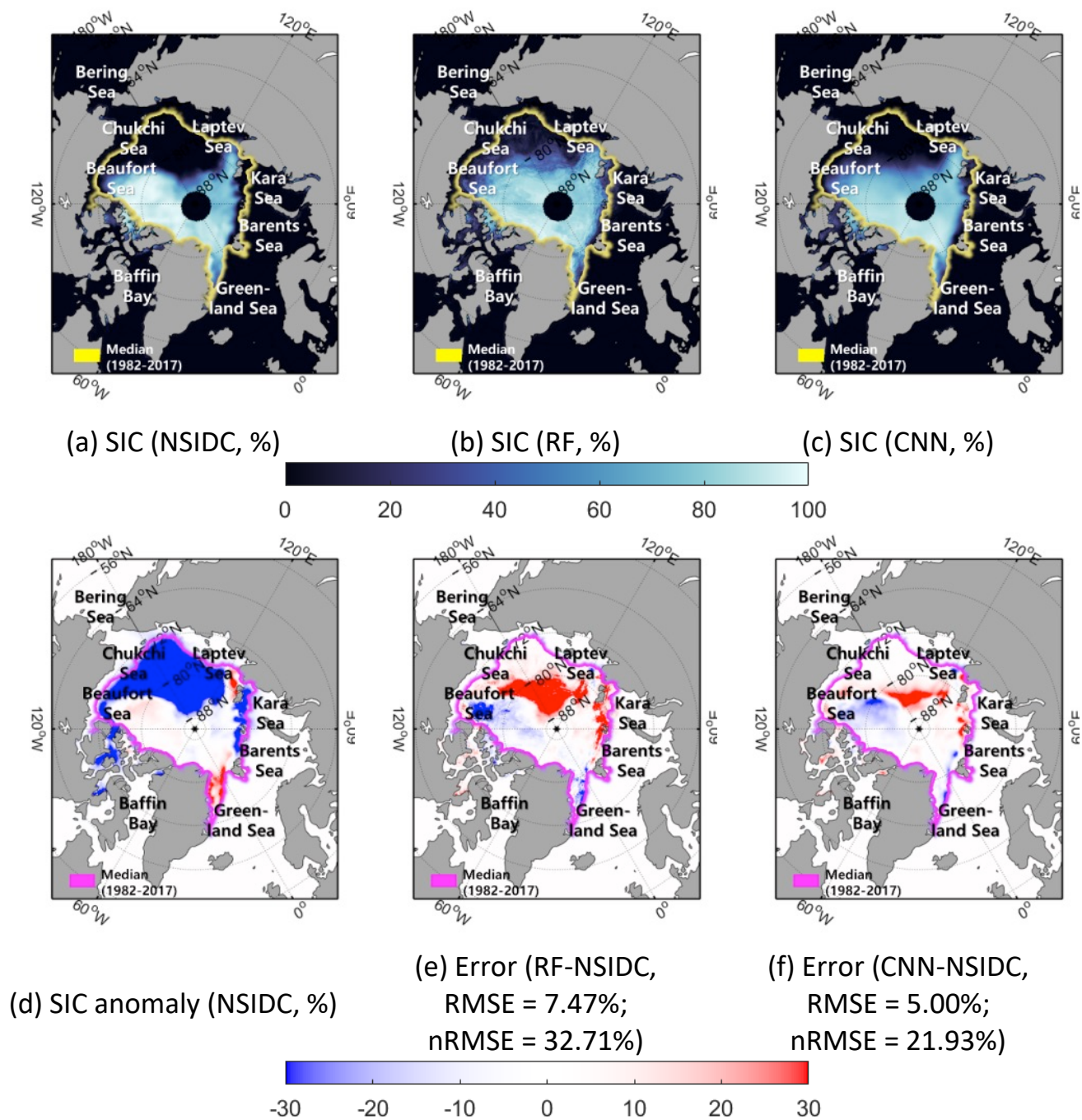
#### 290 4.2 Prediction results in extreme cases: September 2007 and 2012

SIC prediction results of the actual SIC and the SICs predicted by the RF and CNN models were conducted using two extreme cases: September 2007 and 2012 (Fig. 6 and 7). Even though there were unpredicted plummets in the extent the sea ice, the CNN model showed relatively good prediction results in Sep. 2007 and 2012 (RMSE of 5.00 % and 4.71%, nRMSE of 21.93% and 23.95%, respectively).

295 In the case of Sep. 2007, there were large sea ice losses through the Beaufort Sea – Chukchi Sea – Laptev Sea during summer (Fig. 6d). Both the RF and CNN models showed an over-estimation of SIC over the Chukchi Sea and Laptev Sea. This implies that both models were not able to effectively learn the speed of the drastic retreat of sea ice in that region through training (Fig. 6e-f). Similarly, Fig. 7 shows the prediction results and errors based on the RF and the CNN models in Sep. 2012. In summer 2012, there was also a large loss of sea ice over the Beaufort Sea – Laptev Sea – Kara Sea (Fig. 7d). Both the RF and CNN  
300 models yielded over-estimations of SIC in the region between the Barents Sea and the Kara Sea. This might have been caused by the fast decline of sea ice in that region because of warm sea water inflows from the Atlantic Ocean in the summer season (Schauer et al., 2002; Årthun et al., 2012; Kim et al., 2018). The results of two extreme cases showed that the prediction errors



were mainly found in the regions that show high SIC anomalies (i.e., marginal ice zone with small training sample size; Fig. 6d-f and 7d-f).



305

**Figure 6.** The actual SIC (a), predicted SICs (b-c), SIC anomaly (d), and errors between predicted and the actual SICs (e-f) in September 2007.

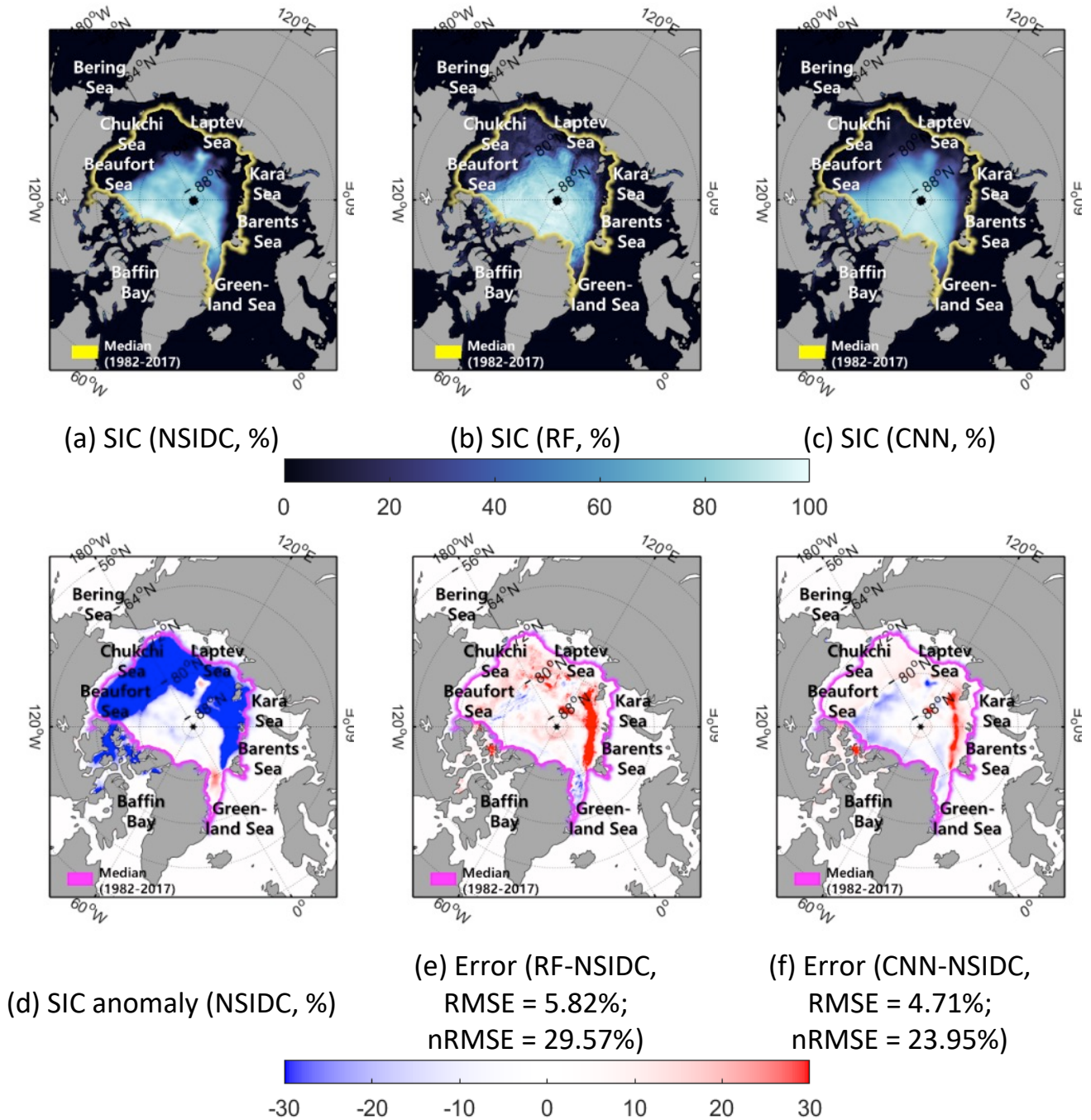


**Figure 7.** The actual SIC (a), predicted SICs (b-c), SIC anomaly (d), and errors between predicted and the actual SICs (e-f) in September 2012.



Together, Figs. 8 and 9 show a detailed analysis focusing on the regions containing high numbers of prediction errors in September 2007 and 2012. Interestingly in both cases, over-estimation was found in no ice zones directly neighboring the marginal sea ice zone (dotted black circle area, Figs. 8 and 9c-d). Both cases show high SST and T2m anomalies together with a low FAL anomaly, caused by a melted snow layer (Figs. 8 and 9i-k). Those anomalous patterns of SST, T2m, and FAL were caused by anomalous strong solar radiation for both cases (Kauker et al., 2009; Kay et al., 2008; Parkinson and Comiso, 2012; Zhang et al., 2013). In regards to v-wind, anomalous warm wind toward the Arctic center, inflowed by strong southerly winds driven from the Pacific water, resulted in melting in the Beaufort Sea in 2007 (Zhang et al., 2008, Fig. 7l). However, the CNN model did not catch the past negative SIC anomalies effectively. For instance, Figs. 8d and h depict overestimation errors in the northern part of the region by showing negative SIC anomalies. Similarly, Figs. 9d, g, and h document over-estimations in the northern part of the region that shows negative SIC anomalies near the Barents Sea and the Kara Sea. Such over-estimation might be caused by the use of a small moving window (i.e., 11-by-11). Since the anomalies were found quite far from the marginal sea ice zone, the models were not able to predict changes in sea ice well. However, a larger window size might impede the overall performance of the model by forcing it to deal with too much learnable information in the CNN approach (Lai et al., 2015). A detailed exploration on the optimum window size is needed in future research.

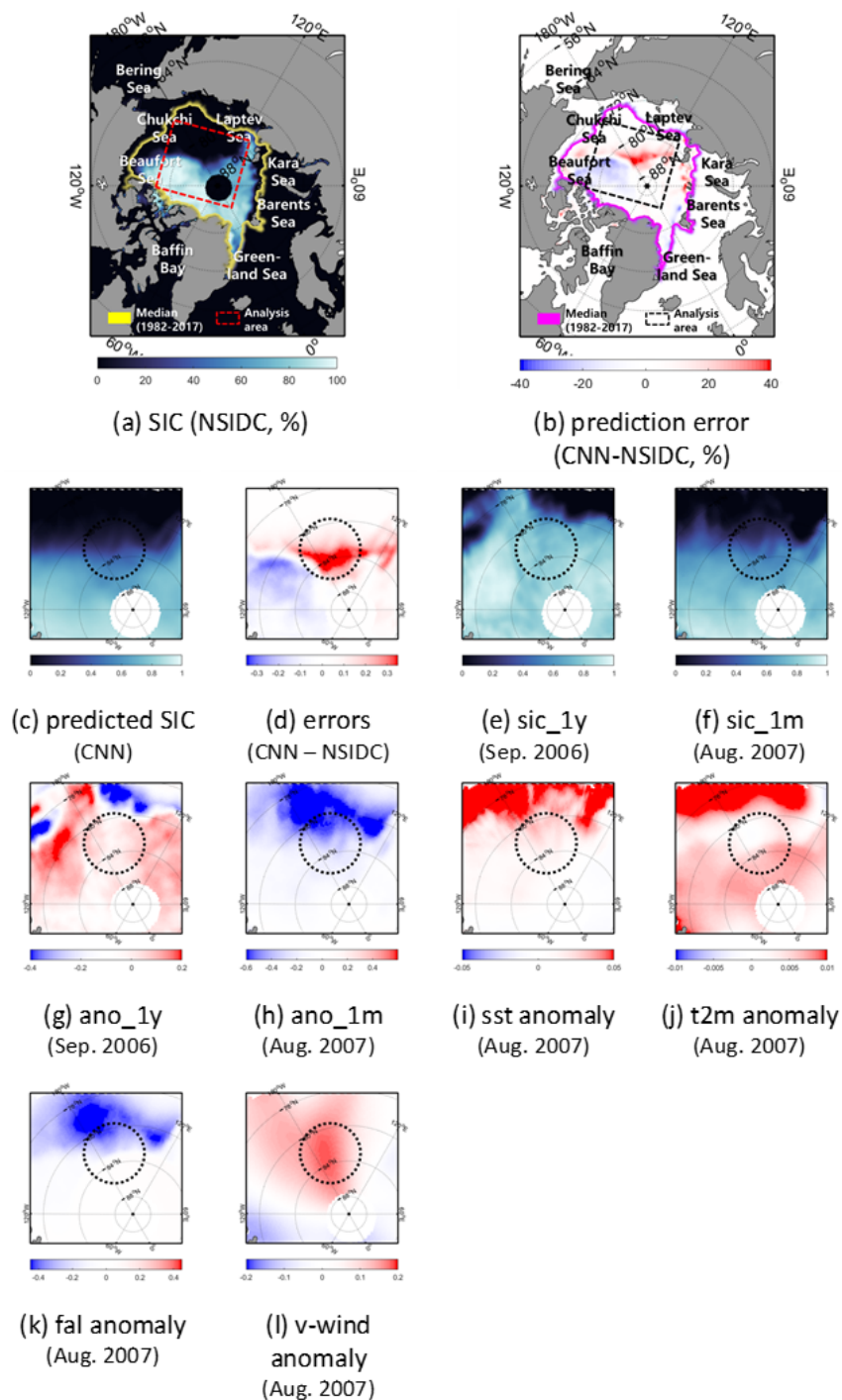
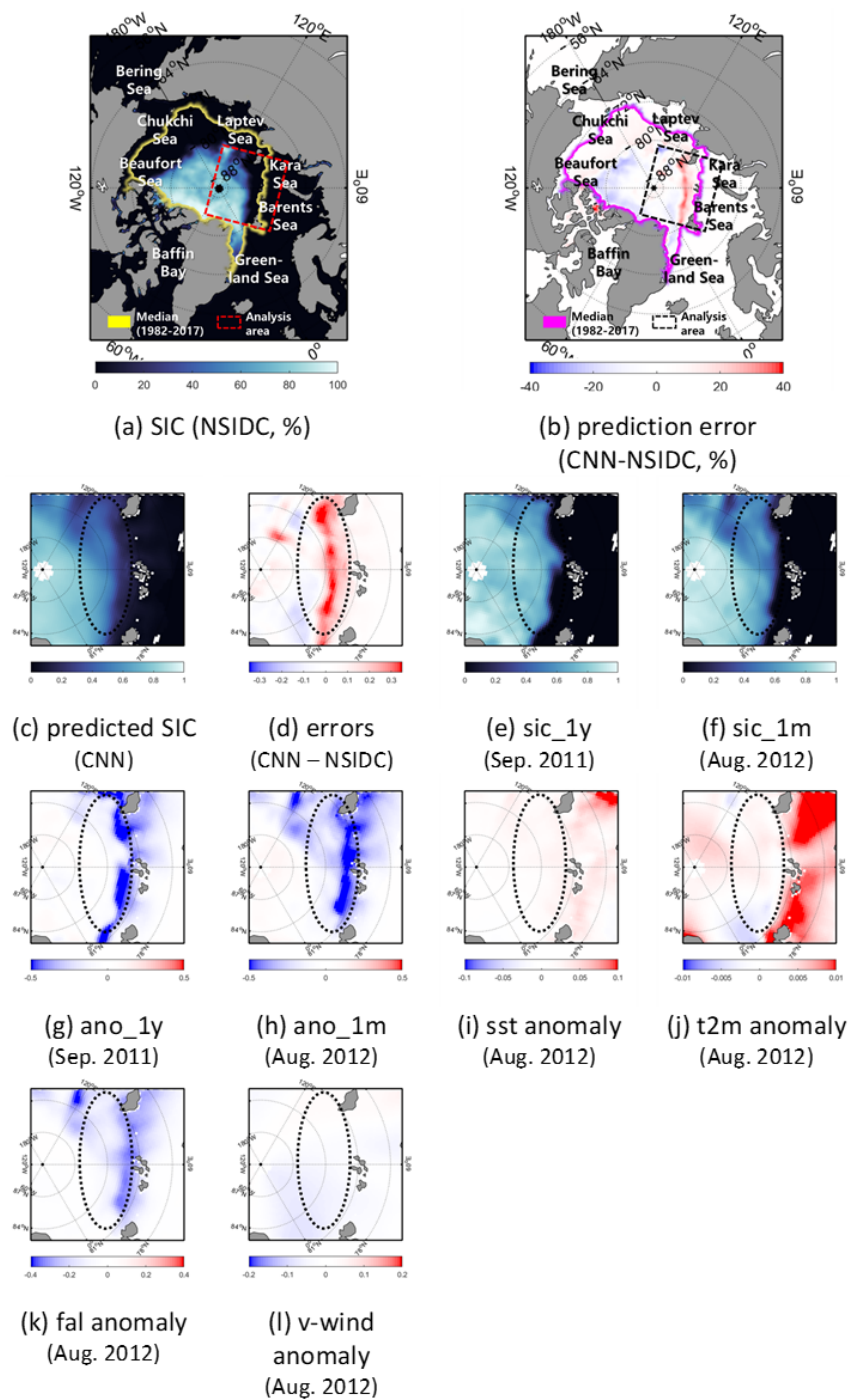


**Figure 8.** Comparison of the prediction results of both models with eight input variables in the Beaufort Sea–Laptev Sea in September 2007. Dotted black circle: the region shows higher prediction error.



330 **Figure 9.** Comparison of the prediction results of both models with eight input variables in the Barents Sea –Kara Sea in September 2012. Dotted black circle: the region shows higher prediction error.



### 4.3 Variable sensitivity

Table 3 shows the variable sensitivity results of both models during 2000-2017. The two models show SIC-related variables as the most sensitive factor, i.e. sic\_1m and sic\_1y, rather than other oceanic or climate variables. These results are consistent for each model in the annual mean, freezing season (Dec.-Mar.), and melting season (Jun.-Sep.). As the SIC-related variables have a role regarding the time-series climatology information of sea ice, SICs themselves can affect SIC prediction in the future (Deser and Teng, 2008; Chi and Kim, 2017). Between long-term climatologies (sic\_1y and ano\_1y) and short-term climatologies (sic\_1m and ano\_1m), the former showed higher sensitivity in both models (except sic\_1y and sic\_1m in the RF). The previous studies have revealed the clear yearly sea ice trends of each month by investigating monthly averaged sea ice extents of the nine Arctic regions and the total from 1979 (Cavalieri and Parkinson, 2012; Parkinson and Cavalieri, 2002). Thus, the monthly models showed long-term climatologies as more contributing factors than the other variables (i.e., SICs in past Jan. is important in the Jan. prediction model). Although long-term climatologies were important in the monthly models, the RF model identified sic\_1m as a most contributing factor than sic\_1y. It might be due to the limitation of the input variables of the RF model used in this study, resulting in a lack of detailed spatial information. The RF model considered spatial information based on 24 additional proxies using an 11-by-11 window (i.e., mean, minimum, and maximum). However, in may not be sufficient to examine the various spatial distributions of input variables. As a result, the RF model might be highly influenced by short-term information rather than long-term variables.

**Table 3.** The average variable sensitivity for the RF and CNN models during 2000-2017 (annual mean, freezing season (Dec.-Mar.), and melting season (Jun.-Sep.)).

		sic_1y	sic_1m	ano_1y	ano_1m	SST	T2m	FAL	v-wind
RF	Annual mean	1.098	<b>1.107</b>	1.086	1.032	1.059	1.029	1.080	1.018
	Freezing season	1.080	<b>1.091</b>	1.087	1.045	1.053	1.011	1.071	1.019
	Melting season	1.098	<b>1.104</b>	1.099	1.031	1.045	1.060	1.079	1.034
CNN	Annual mean	<b>1.134</b>	1.029	1.095	1.012	1.035	1.005	1.006	1.008
	Freezing season	<b>1.145</b>	1.063	1.113	1.026	1.042	1.024	1.015	1.026
	Melting season	<b>1.121</b>	1.033	1.090	1.017	1.054	1.010	1.005	1.015

*The highest value is highlighted*

### 4.4 Variable sensitivity in extreme case: September 2007 and 2012

Table 4 shows the variable sensitivity focusing on every September in 2000-2017, 2007, and 2012. Unlike from the results in Table 3, T2m and FAL were identified as the most influencing factors in the RF model. As reported in many studies, solar radiation has a large effect on the changes in sea ice (Kang et al., 2014; Guemas et al., 2016). In addition, the ice-albedo



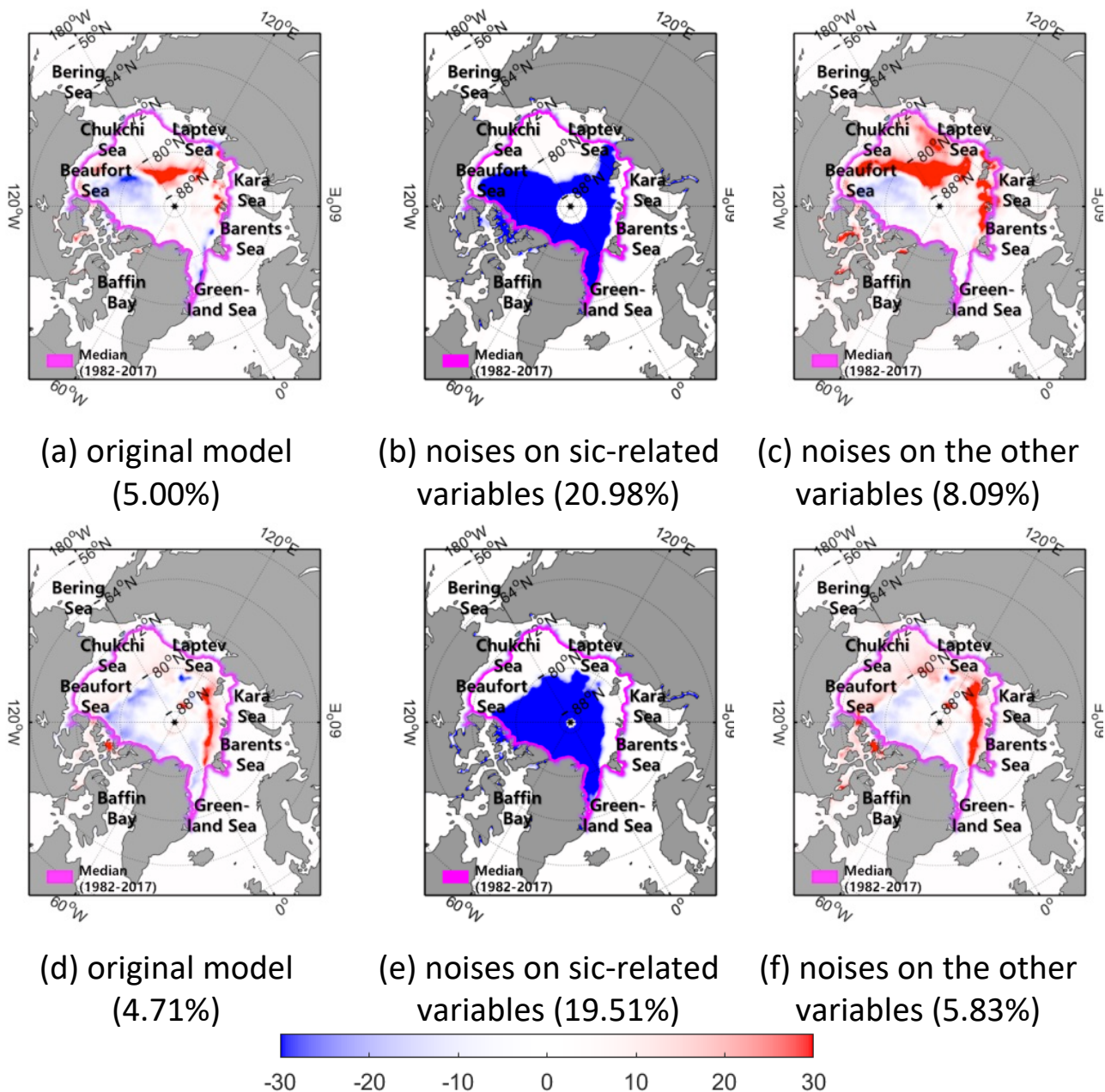
feedback contributes to the recovery of sea ice from the losses in summer (Comiso, 2006; Tietsche et al., 2011). In case of  
 355 September 2007, the warm surface air temperature was the main cause of the drastic decrease of sea ice (Kauker et al., 2009).  
 However, in the case of v-wind, a Gaussian noise made an improvement to the prediction accuracy in two extreme cases for  
 the RF model. While there are no studies revealing the effects of v-wind in Sep. 2012, there is an indirect effect from the  
 southerly warm wind toward the Arctic center in Sep. 2007 (Zhang et al., 2008). Moreover, in the RF model, the degree of  
 sensitivity of FAL is bigger in the two extreme cases than for the entire period. These pieces of evidence may point out that  
 360 the RF model is less robust than the CNN model to highly anomalous SIC cases. In contrast to the RF model, the CNN model  
 consistently identified the sic\_1y as the most contributing variable. Although there is no clear causality between the SICs one-  
 year before and the anomalous decline of sea ice in Sep. 2007 and 2012, past SICs provide information on SICs in future as  
 time-series data (Chi and Kim, 2017).

**Table 4.** The average relative variable importance for the RF and CNN models in September (2000-2017 average, 2007, and 2012).

		sic_1y	sic_1m	ano_1y	ano_1m	SST	T2m	FAL	v-wind
RF	Average	1.095	1.069	1.137	1.067	1.072	1.148	<b>1.165</b>	1.070
	2007	1.136	1.122	1.177	1.118	1.225	<b>1.258</b>	1.207	0.996
	2012	1.126	1.057	1.102	1.064	1.096	1.100	<b>1.207</b>	0.997
CNN	Average	<b>1.090</b>	1.035	1.056	1.005	1.009	1.000	1.002	1.004
	2007	<b>1.133</b>	1.046	1.091	1.022	1.017	1.007	1.008	1.015
	2012	<b>1.078</b>	1.054	1.041	1.020	1.040	1.034	1.023	1.028

*The highest value is highlighted*

365 Figure 10 shows the spatial influence of two sets of variables with impulse noise (zero values). As shown in Figs. 10b and e,  
 the CNN model was not able to predict SICs in the existing sea ice area when using zero values for the SIC-related variables  
 (sic\_1y, sic\_1m, ano\_1y, and ano\_1m). When the CNN model set zero values for the other environmental variables (SST,  
 T2m, FAL, and v-wind), the model was not able to predict a decrease of SICs around the marginal areas between the sea ice  
 and open sea (Fig. 10c and f). It is possibly due to decays on marginal ice zone by anomalous SST, T2m, and FAL in both  
 370 cases. Consistent with the results of the sensitivity analysis (Table 4), SIC-related variables were identified as important  
 indicators to predict SICs (Deser and Teng, 2008). The other meteorological and oceanographic variables tended to affect the  
 SIC changes of the marginal zone ice, particularly, the neighboring thin ice and no ice zone (Stroeve et al., 2008; Chevallier  
 et al., 2013; Zhang et al., 2013).



375 **Figure 10.** The prediction errors (predictions by CNN – NSIDC, %) and RMSE (%) from three prediction results in (a-c) September 2007 (d-f) and 2012: (a and d) original model, (b and e) with noises on SIC variables (sic\_1y, sic\_1m, ano\_1y, and ano\_1m), (c and f) with noises on the other variables.



#### 4.5 Novelty and limitations

Our study developed a novel one-month SIC prediction model using the CNN deep learning approach. The research findings from this study can make a contribution towards filling the gaps in the research on short-term sea ice change and prediction (Grumbine, 1998; Preller and Posey, 1989). Our short-term SIC prediction model can provide valuable information, which can be used in various decision-making processes in the maritime industry and in research regarding sea ice forecasting (Schweiger and Zhang, 2015). Notably, the non-linear learning architectures of the CNN model showed good prediction accuracy based on the larger learning capacity and more consistent temporal SIC prediction than the traditional machine learning approach (Wang et al., 2016; Liu et al., 2018).

However, there are some challenging limitations to the proposed CNN model, particularly regarding the prediction variables. First, this study did not consider the effects of longer time scale, or persistent effects, on sea ice changes (Guemas et al., 2014). For example, the 2007 and 2012 sea ice minimums were caused by not only the anomalous warm atmospheric conditions of the summer season, but also by persistently warm winter and spring seasons, which especially affected the melting in the marginal ice zone (Devasthale et al., 2013). Second, the sea ice thickness is an important factor when predicting sea ice changes because the thinner sea ice is relatively vulnerable to melt (Stroeve et al., 2008; Chevallier et al., 2013; Zhang et al., 2013). However, we did not consider sea ice thickness data because of the limited availability of reliable sea ice thickness products. Third, there is a well-known problem with deep-learning models — interpretability. Because of complicated and non-linear connections between hidden layers, the deep learning models are hard to interpret (Koh et al., 2017; Guidotti et al., 2018). Recent deep learning studies have tried to report explainable results using various visualization approaches such as heat maps and occlusion maps (Brahimi et al., 2017; Trigueros et al., 2018). The present study explained the model using a variable sensitivity analysis, as well as the inspection of the spatial distribution. However, the model still has problems providing clear interpretations of the non-linear relationships among variables.

#### 5. Conclusion

The main purpose of this study was to develop a novel one-month SIC prediction model using the CNN approach. The CNN model showed better prediction performance (MAE of 2.28%, RMSE of 5.76%, nRMSE of 16.15%, and NSE of 0.97) than the simple prediction (MAE of 9.36%, RMSE of 21.93%, nRMSE of 61.94%, and NSE of 0.83) and RF models (MAE of 2.45%, RMSE of 6.61%, nRMSE of 18.64%, and NSE of 0.96). The prediction accuracy in the melting season (Jun. – Sep., nRMSE of 19.09%) was lower than the freezing season (Dec. – Mar., nRMSE of 14.08%). The overall prediction accuracy decreased in the more recent years because of the accelerated sea ice melting caused by global warming. In two extreme cases, the CNN model yielded promising prediction results in respect to RMSE, as well as the spatial distribution of SICs (less than 5% RMSE). The prediction errors normally occurred in the marginal ice zone, which has higher sea ice anomalies. From the variable sensitivity analysis using CNN, the SICs one-year before was identified as the most important factor in predicting sea



ice changes. While the SIC-related variables had high effects on SIC prediction over ice-covered areas, the other  
410 meteorological and oceanographic variables were more sensitive in predicting the SICs in marginal ice zones.

### Acknowledgement

This study was supported by the Korea Polar Research Institute (KOPRI) Grant PE19900 (Development of algorithms to extract satellite-based Arctic sea ice characteristics).

### References

- 415 All About Glaciers, National Snow and Ice Data Center. <https://nsidc.org/cryosphere/glaciers>. Accessed 10 November 2018.
- Årthun, M., Eldevik, T., Smedsrud, L. H., Skagseth, Ø. and Ingvaldsen, R. B.: Quantifying the Influence of Atlantic Heat on Barents Sea Ice Variability and Retreat, *J. Clim.*, 25(13), 4736–4743, doi:10.1175/JCLI-D-11-00466.1, 2012.
- Browne, M. and Ghidary, S. S.: Convolutional neural networks for image processing: an application in robot vision, in *Australasian Joint Conference on Artificial Intelligence*, pp. 641–652., 2003.
- 420 Cavalieri, D. J., C. L. Parkinson, P. Gloersen, and H. J. Zwally: Sea Ice Concentrations from Nimbus-7 SMMR and DMSP SSM/I-SSMIS Passive Microwave Data, Version 1., Boulder, Colorado USA. NASA National Snow and Ice Data Center Distributed Active Archive Center, <https://doi.org/10.5067/8GQ8LZQVL0VL>. 2018.
- Cavalieri, D. J. and Parkinson, C. L.: Arctic sea ice variability and trends, 1979–2010, *The Cryosphere*, 6, 881–889, doi.org/10.5194/tc-6-881-2012, 2012.
- 425 Chen, K., Wang, J., Chen, L.-C., Gao, H., Xu, W. and Nevatia, R.: Abc-cnn: An attention based convolutional neural network for visual question answering, *arXiv Prepr. arXiv1511.05960*, 2015.
- Chi, J. and Kim, H.: Prediction of Arctic Sea Ice Concentration Using a Fully Data Driven Deep Neural Network, *Remote Sens.*, 9(12), 1305, doi:10.3390/rs9121305, 2017.
- Chu, C., Chen, C., Nolte, L. P. and Zheng, G.: Fully automatic cephalometric x-ray landmark detection using random forest regression and sparse shape composition, *Submitt. to Autom. Cephalometric X-ray Landmark Detect. Chall.*, 2014.
- 430 Cohen, J., Screen, J. A., Furtado, J. C., Barlow, M., Whittleston, D., Coumou, D., Francis, J., Dethloff, K., Entekhabi, D., Overland, J. and others: Recent Arctic amplification and extreme mid-latitude weather, *Nat. Geosci.*, 7(9), 627, doi:10.1038/ngeo2234, 2014.
- Comeau, D., Giannakis, D., Zhao, Z. and Majda, A. J.: Predicting regional and pan-Arctic sea ice anomalies with kernel analog forecasting, *Clim. Dyn.*, 52(9–10), 5507–5525, doi:10.1007/s00382-018-4459-x, 2019.
- 435 Comiso, J. C.: Abrupt decline in the Arctic winter sea ice cover, *Geophys. Res. Lett.*, 33(18), doi:10.1029/2006GL027341, 2006.



- Crane, R. G.: Seasonal variations of sea ice extent in the Davis Strait-Labrador Sea area and relationships with synoptic-scale atmospheric circulation, *Arctic*, 434–447, doi:10.14430/arctic2671, 1978.
- 440 Deng, L., Hinton, G. and Kingsbury, B.: New types of deep neural network learning for speech recognition and related applications: An overview, in 2013 IEEE International Conference on Acoustics, Speech and Signal Processing, pp. 8599–8603., 2013.
- Deser, C. and Teng, H.: Evolution of Arctic sea ice concentration trends and the role of atmospheric circulation forcing, 1979–2007, *Geophys. Res. Lett.*, 35(2), doi:10.1029/2007GL032023, 2008.
- 445 Deser, C., Tomas, R. A. and Peng, S.: The transient atmospheric circulation response to North Atlantic SST and sea ice anomalies, *J. Clim.*, 20(18), 4751–4767, doi:doi.org/10.1175/JCLI4278.1, 2007.
- Devasthale, A., Sedlar, J., Koenigk, T. and Fetzer, E. J.: The thermodynamic state of the Arctic atmosphere observed by AIRS: comparisons during the record minimum sea ice extents of 2007 and 2012, *Atmos. Chem. Phys.*, 13(15), 7441–7450, doi:10.5194/acp-13-7441-2013, 2013.
- 450 Dokken, T. M. and Jansen, E.: Rapid changes in the mechanism of ocean convection during the last glacial period, *Nature*, 401(6752), 458, doi:10.1038/46753, 1999.
- Doney, S. C., Ruckelshaus, M., Emmett Duffy, J., Barry, J. P., Chan, F., English, C. A., Galindo, H. M., Grebmeier, J. M., Hollowed, A. B., Knowlton, N. and others: Climate change impacts on marine ecosystems, *Ann. Rev. Mar. Sci.*, 4, 11–37, doi:10.1146/annurev-marine-041911-111611, 2012.
- 455 Emery, W. J., Fowler, C. W. and Maslanik, J. A.: Satellite-derived maps of Arctic and Antarctic sea ice motion: 1988 to 1994, *Geophys. Res. Lett.*, 24(8), 897–900, doi:10.1029/97gl00755, 1997.
- Forkuor, G., Dimobe, K., Serme, I. and Tondoh, J. E.: Landsat-8 vs. Sentinel-2: examining the added value of sentinel-2’s red-edge bands to land-use and land-cover mapping in Burkina Faso, *GIScience Remote Sens.*, 55(3), 331–354, doi:10.1080/15481603.2017.1370169, 2018.
- 460 Francis, J. A. and Vavrus, S. J.: Evidence for a wavier jet stream in response to rapid Arctic warming, *Environ. Res. Lett.*, 10(1), 14005, doi:10.1088/1748-9326/10/1/014005, 2015.
- Fritzner, S., Graversen, R., Christensen, K. H., Rostosky, P. and Wang, K.: Impact of assimilating sea ice concentration, sea ice thickness and snow depth in a coupled ocean–sea ice modelling system, *Cryosph.*, 13(2), 491–509, doi:10.5194/tc-13-491-2019, 2019.
- 465 Ghimire, B., Rogan, J. and Miller, J.: Contextual land-cover classification: incorporating spatial dependence in land-cover classification models using random forests and the Getis statistic, *Remote Sens. Lett.*, 1(1), 45–54, doi:10.1080/01431160903252327, 2010.
- Grumbine, R. W.: Virtual floe ice drift forecast model intercomparison, *Weather Forecast.*, 13(3), 886–890, doi:10.1175/1520-0434(1998)013<0886:VFIDFM>2.0.CO;2, 1998.



- 470 Guemas, V., Blanchard-Wrigglesworth, E., Chevallier, M., Day, J. J., Déqué, M., Doblas-Reyes, F. J., Fučkar, N. S., Germe, A., Hawkins, E., Keeley, S. and others: A review on Arctic sea-ice predictability and prediction on seasonal to decadal time-scales, *Q. J. R. Meteorol. Soc.*, 142(695), 546–561, doi:10.1002/qj.2401, 2016.
- Guidotti, R., Monreale, A., Ruggieri, S., Turini, F., Giannotti, F. and Pedreschi, D.: A survey of methods for explaining black box models, *ACM Comput. Surv.*, 51(5), 93, doi:10.1145/3236009, 2018.
- 475 Guo, Z. and Du, S.: Mining parameter information for building extraction and change detection with very high-resolution imagery and GIS data, *GIScience Remote Sens.*, 54(1), 38–63, doi:10.1080/15481603.2016.1250328, 2017.
- Hassol, S.: Impacts of a warming Arctic-Arctic climate impact assessment, Cambridge University Press., 2004.
- Holland, M. M. and Stroeve, J.: Changing seasonal sea ice predictor relationships in a changing Arctic climate, *Geophys. Res. Lett.*, 38(18), doi:10.1029/2011gl049303, 2011.
- 480 Johannessen, O. M., Bengtsson, L., Miles, M. W., Kuzmina, S. I., Semenov, V. A., Alekseev, G. V., Nagurnyi, A. P., Zakharov, V. F., Bobylev, L. P., Pettersson, L. H. and others: Arctic climate change: observed and modelled temperature and sea-ice variability, *Tellus A Dyn. Meteorol. Oceanogr.*, 56(4), 328–341, doi:10.3402/tellusa.v56i5.14599, 2004.
- Kauker, F., Kaminski, T., Karcher, M., Giering, R., Gerdes, R. and Voßbeck, M.: Adjoint analysis of the 2007 all time Arctic sea-ice minimum, *Geophys. Res. Lett.*, 36(3), doi:10.1029/2008gl036323, 2009.
- 485 Kay, J. E., L’Ecuyer, T., Gettelman, A., Stephens, G. and O’Dell, C.: The contribution of cloud and radiation anomalies to the 2007 Arctic sea ice extent minimum, *Geophys. Res. Lett.*, 35(8), doi:10.1029/2008gl033451, 2008.
- Kern, S., Rösel, A., Pedersen, L. T., Ivanova, N., Saldo, R. and Tonboe, R. T.: The impact of melt ponds on summertime microwave brightness temperatures and sea-ice concentrations, *Cryosph.*, 10(5), 2217–2239, doi:10.5194/tc-10-2217-2016, 2016.
- 490 Kim, J., Kim, K., Cho, J., Kang, Y., Yoon, H.-J. and Lee, Y.-W.: Satellite-Based Prediction of Arctic Sea Ice Concentration Using a Deep Neural Network with Multi-Model Ensemble, *Remote Sens.*, 11(1), 19, doi:10.3390/rs11010019, 2019.
- Koh, P. W. and Liang, P.: Understanding black-box predictions via influence functions, in *Proceedings of the 34th International Conference on Machine Learning-Volume 70*, pp. 1885–1894., 2017.
- Krizhevsky, A., Sutskever, I. and Hinton, G. E.: Imagenet classification with deep convolutional neural networks, in *Advances in neural information processing systems*, pp. 1097–1105., 2012.
- 495 Lai, S., Xu, L., Liu, K. and Zhao, J.: Recurrent convolutional neural networks for text classification, in *Twenty-ninth AAAI conference on artificial intelligence.*, 2015.
- LeCun, Y., Bottou, L., Bengio, Y. and Haffner, P.: Gradient-based learning applied to document recognition, *Proc. IEEE*, 86(11), 2278–2324, 1998.
- 500 Ledley, T. S.: A coupled energy balance climate-sea ice model: Impact of sea ice and leads on climate, *J. Geophys. Res. Atmos.*, 93(D12), 15919–15932, doi:10.1029/jd093id12p15919, 1988.



- Lee, H., Grosse, R., Ranganath, R. and Ng, A. Y.: Convolutional deep belief networks for scalable unsupervised learning of hierarchical representations, in Proceedings of the 26th annual international conference on machine learning, pp. 609–616., 2009.
- 505 Liu, T., Abd-Elrahman, A., Jon, M. and Wilhelm, V. L.: Comparing Fully Convolutional Networks, Random Forest, Support Vector Machine, and Patch-based Deep Convolutional Neural Networks for Object-based Wetland Mapping using Images from small Unmanned Aircraft System, *GIScience Remote Sens.*, (just-accepted), doi:10.1080/15481603.2018.1426091, 2018.
- Mahajan, S., Zhang, R. and Delworth, T. L.: Impact of the Atlantic meridional overturning circulation (AMOC) on Arctic surface air temperature and sea ice variability, *J. Clim.*, 24(24), 6573–6581, doi:10.1175/2011jcli4002.1, 2011.
- 510 Maslanik, J. A., Fowler, C., Stroeve, J., Drobot, S., Zwally, J., Yi, D. and Emery, W.: A younger, thinner Arctic ice cover: Increased potential for rapid, extensive sea-ice loss, *Geophys. Res. Lett.*, 34(24), doi:10.1029/2007gl032043, 2007.
- Melia, N., Haines, K. and Hawkins, E.: Sea ice decline and 21st century trans-Arctic shipping routes, *Geophys. Res. Lett.*, 43(18), 9720–9728, doi:10.1002/2016gl069315, 2016.
- Moriassi, D. N., Arnold, J. G., Van Liew, M. W., Bingner, R. L., Harmel, R. D., and Veith, T. L. : Model evaluation guidelines  
515 for systematic quantification of accuracy in watershed simulations, *T. ASABE.*, 50(3), 885-900, doi: 10.13031/2013.23153, 2007.
- Mutanga, O., Adam, E. and Cho, M. A.: High density biomass estimation for wetland vegetation using WorldView-2 imagery and random forest regression algorithm, *Int. J. Appl. Earth Obs. Geoinf.*, 18, 399–406, doi:10.1016/j.jag.2012.03.012, 2012.
- Nash, J. E., and Sutcliffe, J. V. : River flow forecasting through conceptual models part I—A discussion of principles, *J.*  
520 *Hydrol.*, 10(3), 282-290, doi : 10.1016/0022-1694(70)90255-6, 1970.
- Open University: *Ocean Circulation (Second Edition)*, Second Edi., Butterworth-Heinemann, Oxford., 2001.
- Parkinson, C. L., and Cavalieri, D. J.: A 21 year record of Arctic sea-ice extents and their regional, seasonal and monthly variability and trends, *Ann. Glaciol.*, 34, 441-446, doi.org/10.3189/172756402781817725, 2002.
- Parkinson, C. L. and Comiso, J. C.: On the 2012 record low Arctic sea ice cover: Combined impact of preconditioning and an  
525 August storm, *Geophys. Res. Lett.*, 40(7), 1356–1361, doi:10.1002/grl.50349, 2013.
- Prasad, S., Zakharov, I., McGuire, P., Power, D. and Richard, M.: Estimation of sea ice parameters from sea ice model with assimilated ice concentration and SST, *Cryosph.*, 12(12), 3949–3965, doi:10.5194/tc-2018-112, 2018.
- Preller, R. H. and Posey, P. G.: *The polar ice prediction system—a sea ice forecasting system.*, 1989.
- Rayner, N. A. A., Parker, D. E., Horton, E. B., Folland, C. K., Alexander, L. V, Rowell, D. P., Kent, E. C. and Kaplan, A.:  
530 *Global analyses of sea surface temperature, sea ice, and night marine air temperature since the late nineteenth century*, *J. Geophys. Res. Atmos.*, 108(D14), doi:10.1029/2002jd002670, 2003.
- Ren, S., He, K., Girshick, R. and Sun, J.: Faster r-cnn: Towards real-time object detection with region proposal networks, in *Advances in neural information processing systems*, pp. 91–99., 2015.



- Richardson, H. J., Hill, D. J., Denesiuk, D. R. and Fraser, L. H.: A comparison of geographic datasets and field measurements  
535 to model soil carbon using random forests and stepwise regressions (British Columbia, Canada), *GIScience Remote Sens.*,  
54(4), 573–591, doi:10.1080/15481603.2017.1302181, 2017.
- Rodner, E., Simon, M., Fisher, R. B. and Denzler, J.: Fine-grained recognition in the noisy wild: Sensitivity analysis of  
convolutional neural networks approaches, *arXiv Prepr. arXiv1610.06756*, 2016.
- Schauer, U., Loeng, H., Rudels, B., Ozhigin, V. K., and Dieck, W.: Atlantic water flow through the Barents and Kara Seas.  
540 *Deep Sea Research Part I: Oceanographic Research Papers*, 49(12), 2281–2298, doi.org/10.1016/s0967-0637(02)00125-5,  
2002.
- Schweiger, A. J. and Zhang, J.: Accuracy of short-term sea ice drift forecasts using a coupled ice-ocean model, *J. Geophys.*  
*Res. Ocean.*, 120(12), 7827–7841, doi:10.1016/s0967-0637(02)00125-5, 2015.
- Schweiger, A. J., Zhang, J., Lindsay, R. W. and Steele, M.: Did unusually sunny skies help drive the record sea ice minimum  
545 of 2007?, *Geophys. Res. Lett.*, 35(10), doi:doi.org/10.1029/2008gl033463, 2008.
- Screen, J. A. and Simmonds, I.: The central role of diminishing sea ice in recent Arctic temperature amplification, *Nature*,  
464(7293), 1334, doi:10.1038/nature09051, 2010.
- Screen, J. A., Simmonds, I., Deser, C. and Tomas, R.: The atmospheric response to three decades of observed Arctic sea ice  
loss, *J. Clim.*, 26(4), 1230–1248, doi:10.1175/jcli-d-12-00063.1, 2013.
- 550 Shimada, K., Kamoshida, T., Itoh, M., Nishino, S., Carmack, E., McLaughlin, F., Zimmermann, S. and Proshutinsky, A.:  
Pacific Ocean inflow: Influence on catastrophic reduction of sea ice cover in the Arctic Ocean, *Geophys. Res. Lett.*, 33(8),  
doi:10.1029/2005gl025624, 2006.
- Sonobe, R., Yamaya, Y., Tani, H., Wang, X., Kobayashi, N. and Mochizuki, K.: Assessing the suitability of data from Sentinel-  
1A and 2A for crop classification, *GIScience Remote Sens.*, 54(6), 918–938, doi:10.1080/15481603.2017.1351149, 2017.
- 555 Steele, M., Ermold, W. and Zhang, J.: Arctic Ocean surface warming trends over the past 100 years, *Geophys. Res. Lett.*, 35(2),  
doi:10.1029/2007gl031651, 2008.
- Stroeve, J., Holland, M. M., Meier, W., Scambos, T. and Serreze, M.: Arctic sea ice decline: Faster than forecast, *Geophys.*  
*Res. Lett.*, 34(9), doi.org/10.1029/2007GL029703, 2007.
- Stroeve, J., Hamilton, L. C., Bitz, C. M. and Blanchard-Wrigglesworth, E.: Predicting September sea ice: Ensemble skill of  
560 the SEARCH sea ice outlook 2008–2013, *Geophys. Res. Lett.*, 41(7), 2411–2418, doi:10.1002/2014gl059388, 2014.
- Stroeve, J. C., Serreze, M. C., Holland, M. M., Kay, J. E., Malanik, J. and Barrett, A. P.: The Arctic’s rapidly shrinking sea ice  
cover: a research synthesis, *Clim. Change*, 110(3–4), 1005–1027, doi:10.1007/s10584-011-0101-1, 2012.
- Stroeve, J., Serreze, M., Drobot, S., Gearheard, S., Holland, M., Maslanik, J., Meier, W., and Scambos, T.: Arctic sea ice extent  
plummets in 2007. *Eos, Transactions American Geophysical Union*, 89(2), 13–14, doi.org/10.1029/2008eo020001, 2008.
- 565 Tieleman, T. and Hinton, G.: Lecture 6.5-rmsprop: Divide the gradient by a running average of its recent magnitude,  
*COURSERA Neural networks Mach. Learn.*, 4(2), 26–31, 2012.



- Tietsche, S., Notz, D., Jungclaus, J. H. and Marotzke, J.: Recovery mechanisms of Arctic summer sea ice, *Geophys. Res. Lett.*, 38(2), doi:10.1029/2010gl045698, 2011.
- 570 Timmermann, R., Danilov, S., Schröter, J., Böning, C., Sidorenko, D. and Rollenhagen, K.: Ocean circulation and sea ice distribution in a finite element global sea ice--ocean model, *Ocean Model.*, 27(3–4), 114–129, doi:10.1016/j.ocemod.2008.10.009, 2009.
- Trigueros, D. S., Meng, L., and Hartnett, M.: Enhancing convolutional neural networks for face recognition with occlusion maps and batch triplet loss, *Image Vision Comput.*, 79, 99–108, doi.org/10.1016/j.imavis.2018.09.011, 2018.
- 575 Wang, L., Scott, K. A., Xu, L. and Clausi, D. A.: Sea ice concentration estimation during melt from dual-pol SAR scenes using deep convolutional neural networks: A case study, *IEEE Trans. Geosci. Remote Sens.*, 54(8), 4524–4533, doi:10.1109/tgrs.2016.2543660, 2016.
- Wang, L., Scott, K. and Clausi, D.: Sea ice concentration estimation during freeze-up from SAR imagery using a convolutional neural network, *Remote Sens.*, 9(5), 408, doi:10.3390/rs9050408, 2017.
- 580 Yoo, C., Im, J., Park, S. and Quackenbush, L. J.: Estimation of daily maximum and minimum air temperatures in urban landscapes using MODIS time series satellite data, *ISPRS J. Photogramm. Remote Sens.*, 137, 149–162, doi:10.1016/j.isprsjprs.2018.01.018, 2018.
- Yu, L., Zhong, S., Winkler, J. A., Zhou, M., Lenschow, D. H., Li, B., Wang, X. and Yang, Q.: Possible connections of the opposite trends in Arctic and Antarctic sea-ice cover, *Sci. Rep.*, 7, 45804, doi:10.1038/srep45804, 2017.
- 585 Yuan, X., Chen, D., Li, C., Wang, L. and Wang, W.: Arctic sea ice seasonal prediction by a linear Markov model, *J. Clim.*, 29(22), 8151–8173, doi:10.1175/jcli-d-15-0858.1, 2016.
- Zhang, E., Liu, L., and Huang, L.: Automatically delineating the calving front of Jakobshavn Isbræ from multi-temporal TerraSAR-X images: a deep learning approach, *The Cryosphere Discuss.*, doi.org/10.5194/tc-2019-14, in review, 2019.
- Zhang, J., Lindsay, R., Schweiger, A. and Steele, M.: The impact of an intense summer cyclone on 2012 Arctic sea ice retreat, *Geophys. Res. Lett.*, 40(4), 720–726, doi:10.1002/grl.50190, 2013.